

激光重熔改性铝合金微弧氧化膜层的组织与性能

喻 杰, 韦东波, 王 岩, 吕鹏翔, 狄士春

(哈尔滨工业大学 机电工程学院, 哈尔滨 150001)

摘 要: 为了改善微弧氧化(MAO)膜层多孔疏松的组织 and 性能, 对其进行了激光重熔处理, 并制备了两种实验膜层: (1)选择双向电流脉冲和 $\text{Na}_2\text{SiO}_3\text{-KOH}$ 体系的工作液, 在 6082 铝合金基体上制备平均厚度为 $18\ \mu\text{m}$ 的 MAO 膜层; (2)采用 Nd:YAG 激光器对上述 MAO 膜层进行激光重熔(LSM)处理, 获得 MAO+LSM 膜层。利用扫描电子显微镜(SEM)、X 射线衍射仪、超显微硬度计和电化学分析仪分别检测上述两种膜层的微观形貌、相组成、表面硬度和耐蚀性能。结果表明: 激光重熔后的膜层由内往外分为致密层、中间层和重熔层, 组织致密、气孔率低的重熔层取代了 MAO 疏松层, MAO+LSM 膜层中 $\alpha\text{-Al}_2\text{O}_3$ 相的比例得到提高, 硬度和耐蚀性能也进一步得到改善, 且保持了 MAO 膜层与基体的结合方式。

关 键 词: 铝合金; 微弧氧化; 激光重熔; 耐蚀性

中图分类号: TG174 文献标识码: A

Structure and Property of Micro-arc Oxidation Coating Modified by Laser Melting and Solidifying on Aluminum Alloy

YU Jie, WEI Dong-Bo, WANG Yan, LÜ Peng-Xiang, DI Shi-Chun

(School of Mechatronics Engineering, Harbin Institute of Technology, Harbin 150001, China)

Abstract: In order to improve performance and microstructure of micro-arc oxidation (MAO) coating, especially loose and porous characteristic, a laser melting and solidifying process (LSM) was introduced. Two kinds of samples were prepared: (1) MAO coatings, $18\ \mu\text{m}$ average thickness, were produced on 6082 aluminum alloy by bipolar current pulse in $\text{Na}_2\text{SiO}_3\text{-KOH}$ solution. (2) a melting process using a Nd:YAG laser was employed to modify above-mentioned MAO coatings to obtain MAO+LSM coating. Microstructure of two kinds of coatings (MAO coating and MAO+LSM coating) were examined by scanning electron microscopy. X-ray diffraction was used to determine the phase composition of the coatings. Coating hardness was tested by ultra-micro hardness tester, and corrosion performance was investigated by polarization test instrument. The results show that the MAO+LSM coating is composed of dense layer, intermediate layer and melting layer from inside to surface. The loose layer of MAO film is replaced by a dense and low porosity melting layer after LSM treatment. The occupancy of $\alpha\text{-Al}_2\text{O}_3$ phase in MAO+LSM is improved compared with MAO coating. Hardness and anticorrosion performance of MAO+LSM coating are also further strengthened while the remelted coating keeps the same binding manner as MAO coating.

Key words: 6082 aluminum alloy; micro-arc oxidation; laser melting and solidifying; anticorrosion behavior

铝合金具有重量轻、比强度高、成本低等特点, 被广泛应用于现代工业生产中, 但其硬度、耐磨性

收稿日期: 2012-10-09; 收到修改稿日期: 2012-11-05

作者简介: 喻 杰(1986-), 男, 博士研究生. E-mail: yujie163.ok@163.com

通讯作者: 狄士春, 教授. E-mail: dishichun@126.com

等机械性能和耐蚀性能有待提高^[1-6]。微弧氧化是在电化学反应和等离子放电作用下,在 Al、Mg、Ti 等阀金属及其合金表面原位生长陶瓷膜层的表面改性技术^[6-8]。在众多表面处理技术中,MAO 膜层与基体具有较好的结合力^[9-11],但膜层外部一般为疏松层,内部为致密层,疏松层比致密层厚,组织松散,且主要由硬度较低的 γ - Al_2O_3 组成^[12-14]。MAO 的等离子体放电通道内熔融物喷射淬冷后形成了膜层的多孔结构,随着放电的持续孔径逐渐变大,并且一些较大的孔隙贯通了膜层表面和基体,MAO 膜层的这些特点降低了膜层的耐磨和耐蚀性能^[15]。激光重熔是在激光束热作用下改变材料表面微观结构和相组成,提高材料的耐磨、防腐和抗氧化性能的表面改性技术^[16-18]。许多学者研究表明激光重熔有利于消除材料的缺陷,改善陶瓷体力学性能,重熔和再凝固可实现多孔陶瓷的封孔,膜层表面变得光滑^[19-22]。Mateos 研究等离子喷涂膜层的激光重熔时,发现重熔后大量的孔隙消失,微观组织的一致性也变好^[23]。本工作结合 MAO 和 LSM 两种工艺有望获得结合力好、整体组织致密和硬度高的膜层,提高膜层的防腐和耐磨性能。

1 实验方法

实验样件材料为 6082 铝合金,MAO 样件尺寸:100mm×50mm×4mm。

实验步骤分为两步:

(a)在铝合金基体上制备 MAO 膜层。铝合金样件经 1000#砂纸打磨后,先后在自来水和去离子水中清洗,然后烘干。在 Na_2SiO_3 -KOH 体系的工作液中,对预处理后的铝合金用 MAO 工艺处理 40 min,工作液中各溶质浓度分别为 $C_{\text{Na}_2\text{SiO}_3}=20$ g/L, $C_{\text{KOH}}=1$ g/L 和 $C_{(\text{NaPO}_3)_6}=8$ g/L,溶剂为去离子水,装有工作液的不锈钢槽体为负极,样件为正极,采用双向恒流加工方式,正向电流 10 A,负向电流 4 A,频率 500 Hz,保持电解液温度 30~35℃,电源为哈尔滨迪斯数控设备有限公司研制的 15 kW 微弧氧化实验专用脉冲电源;

(b)激光重熔多孔微弧氧化膜层。利用线切割机将 MAO 样件分割成尺寸为 15 mm×15 mm 的小样件,然后经肥皂水、自来水多次清洗后,最后在酒精中进行超声波清洗 5~10 min,直至表面洁净后烘干。利用 Nd:YAG 激光器对小样件的 MAO 膜层进行重熔处理,优化工艺后,激光重熔参数如下:焦点至膜层表面距离为 12~15 mm,激光功率 23~31 W,

扫描速度 2~6 mm/s,激光扫描重叠率为 50%。

激光器是英国 GUS 公司生产的型号为 LUMONICS JK700。采用美国 FEI 公司生产的 SIRION 扫描电子显微镜(SEM)分析 MAO 和 MAO+LSM 膜层的表面和截面的微观形貌和组织结构。采用日本理学株式会社生产的 D/max-rB 旋转阳极 X 射线衍射仪对 MAO 涂层和 MAO+LSM 膜层的物相成分进行分析。利用日本株式会社生产的岛津 DUH-W201S 型超显微硬度计测量膜层表面硬度。采用上海晨华仪器公司生产的电化学分析仪测定了膜层在 3.5%NaCl 水溶液中的动电位极化曲线。

2 实验结果与讨论

2.1 激光重熔对 MAO 膜层的微观形貌的影响

图 1 是 MAO 膜层和微弧氧化膜层经激光重熔(MAO+LSM)后的表面形貌。MAO 膜层生长主要是在等离子体放电作用下完成的,单次等离子体放电通常经历介电击穿形成放电通道,放电通道附近的金属及其氧化物熔化,在高温和高压的放电通道内的熔融物往外喷射,在工作液中淬冷后,膜层表面形成大量的“火山口”,并且“火山口”附近堆积了许多冷却物,形成小突起,且分布大量的微孔,膜层也因此而变得粗糙,如图 1(a)和图 1(b)所示。MAO 膜层中微孔边沿的小突起为附近区域的“制高点”,如图 1(b)所示,激光束照射到 MAO 膜层后,小突起距离激光焦点距离近而获得激光辐射的能量密度较高,激光束在突起中心的微孔内反复折射后,突起微区辐射的能量密度进一步提高,因此,MAO 膜层在激光重熔过程中先在突起处形成较小熔池,然后熔池逐渐往外生长,相邻熔池的熔融物流动、汇集后形成熔融区,熔融区之间相互连接,在大气环境下冷却后形成表面光滑,微孔稀疏,组织致密的膜层结构,如图 1(c)所示。若照射到膜层激光光斑能量密度较低,扫描速度较快,形成的熔池较小且熔融物保持高温时间短熔池不易长大,难以形成连续的熔融区,重熔后膜层表面间隔地分布着 MAO 和 MAO+LSM 的形貌,如图 1(d)和图 1(e)所示,黑色曲线区域为 LSM+MAO 膜层区域,其余为 MAO 膜层。图 1(f)反映了 MAO 和 MAO+LSM 膜层边界区域的形貌,激光重熔后膜层表面的微孔减少,封孔效果明显,但表面出现凹陷区域,可能为熔池中的熔融物流入较大的 MAO 膜层孔隙,导致其附近出现凹陷,另有边沿规则的圆孔可能为重熔过程中膜层内部的排气通道。

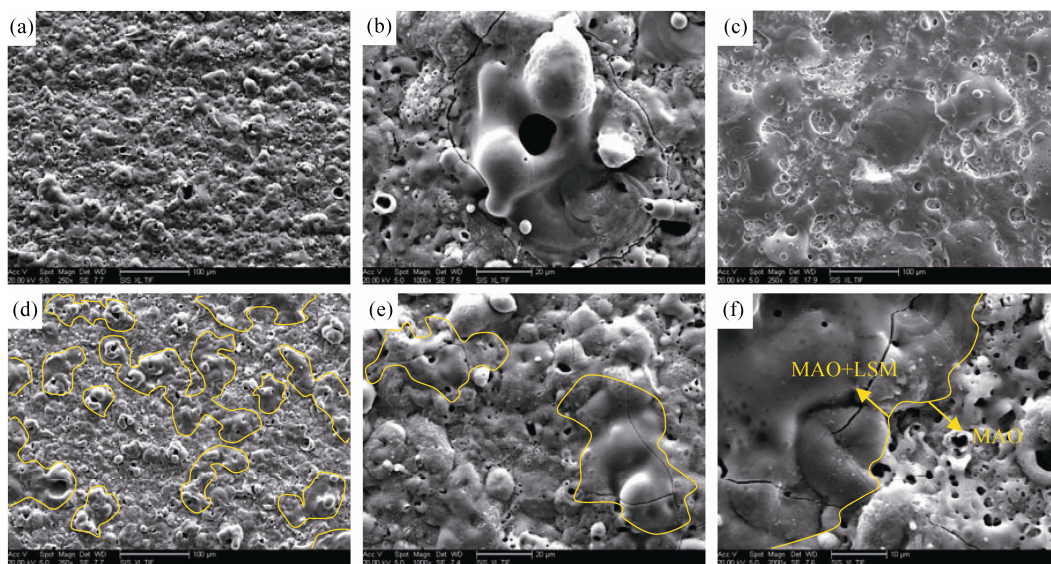


图 1 MAO 和 MAO+LSM 膜层的表面 SEM 照片

Fig. 1 SEM images of MAO and MAO+LSM surface topography

(a) MAO coating; (b) Tower around crate; (c) Continuous MAO+LSM coating; (d,e) Interrupted MAO+LSM coating; (f) Boundary surface micro topography between MAO and MAO+LSM

图 2 为 MAO 和 MAO+LSM 膜层的截面形貌, MAO 膜层内部一般为组织较好的致密层, 但致密层所占整个膜层厚度的比例不高, 外部为疏松多孔, 防腐和耐磨性能较差的疏松层, MAO 膜层内部存在因微弧放电留下的盲孔, 以及贯穿基体和膜层外部的通孔。另外, 放电通道内的高温熔融物喷射后在工作液中淬冷, 产生大量裂纹等组织缺陷, 使得外部疏松层内聚力弱, 容易脱落, 如图 2(a)所示。图 2(b)所示为重熔后的膜层截面形貌, 原 MAO 膜层中致密层组织变化较小, 保留了 MAO 膜层与基体结合力好的优点, 而外部疏松层经激光处理后形成了致密的重熔层, 重熔层内部微孔、裂纹明显减少, 且极大地降低了连通基体和膜层外部通孔出现的几率, 膜层表面的小突起和疏松颗粒减少, 表面变得整

齐、平直。在图 2(b)所示重熔后的膜层中, 激光重熔层和微弧氧化致密层之间有一较窄的中间层, 内含少量的较小孔隙, 此部分在 MAO 膜层中为靠内的疏松层, 在激光热能往膜层内部传递过程中, 热作用逐渐减弱, 激光热源改变膜层组织的能力也随之降低, 因此, 中间层还“继承”了 MAO 疏松层的组织特征, 但该层的存在保护了 MAO 致密层和基体的组织以及二者的结合方式。因此, 根据截面形貌特征可将 MAO+LSM 膜层为三层, 由内往外分别为致密层、中间层和重熔层。

2.2 激光重熔对膜层相组成的影响

在铝合金的 MAO 膜层中, 通常以 $\gamma\text{-Al}_2\text{O}_3$ 和 $\alpha\text{-Al}_2\text{O}_3$ 相为主, $\gamma\text{-Al}_2\text{O}_3$ 和 $\alpha\text{-Al}_2\text{O}_3$ 的相变温度分别为 560°C 和 1370°C 。在此实验条件下制备的 MAO

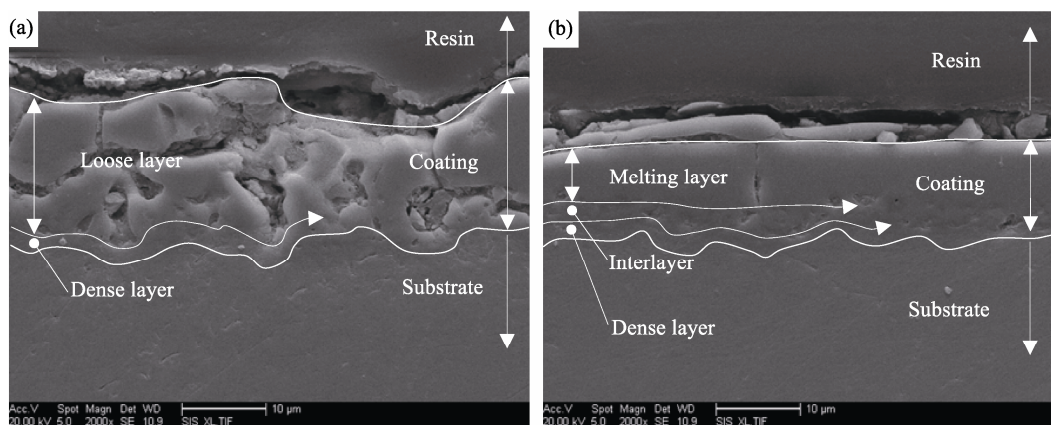


图 2 MAO 和 MAO+LSM 膜层的截面 SEM 照片

Fig. 2 SEM images of MAO and MAO+LSM cross-sectional topography

(a) MAO coating; (b) MAO+LSM coating

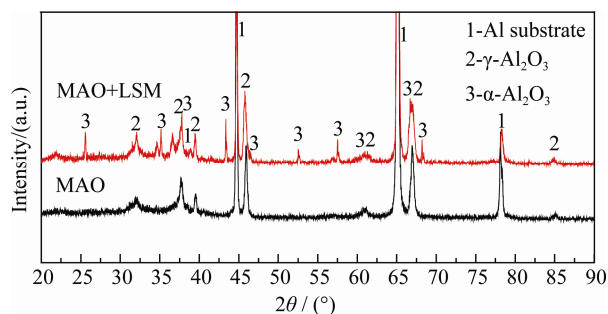


图3 MAO和MAO+LSM膜层XRD图谱

Fig. 3 XRD patterns of the MAO and MAO+LSM samples

样片中,并未检测到含有 α - Al_2O_3 晶相,如图3所示。实验观察和相关研究表明微弧氧化膜层生长前期火花密度大,火花移动速度快,放电通道内能量较小^[24],不易形成较长时间的“高温烧结”环境,故MAO前期难以生成 α - Al_2O_3 。在激光束扫描MAO膜层过程中,具有高能量密度的激光光斑照射到膜层后,其局部区域温度迅速上升至数千摄氏度以致部分膜层融化形成熔池,熔池往基体方向为热传率低的氧化铝陶瓷,外部与大气接触,不同于MAO工艺条件的工作液,周围热绝缘性相对较好的介质有利于保护熔池的高温环境,促进高温区域内熔融物由 γ - Al_2O_3 向 α - Al_2O_3 转变,图3表明激光重熔后出现了高温陶瓷相的 α - Al_2O_3 。相对于MAO过程大部分能量迅速传递给工作液,LSM过程中能量利用率较高。

2.3 激光重熔对膜层硬度的影响

铝合金基体、MAO和MAO+LSM膜层的表面硬度值见表1。基体的显微硬度为105.324 HV,MAO和MAO+LSM膜层的硬度分别为432.022 HV和962.768 HV,相比基体的硬度均有较大提高。而MAO膜层经激光重熔和重结晶后具有更好的硬度:一方面,由于激光重熔提高了MAO膜层中高硬度 α - Al_2O_3 的比例;另一方面,激光重熔后外部膜层组织由疏松多孔变得致密、紧凑、孔隙率低,大幅增加了具有致密组织的膜层厚度,提高了膜层的内聚力。

表1 基体、MAO和MAO+LSM膜层的硬度和极化参数
Table 1 Vickers hardness and polarisation data of substrate, MAO and MAO+LSM coating

Coating Process	HV/(kg·mm ⁻²)	Corrosion current density/(nA·cm ⁻²)	Corrosion potential/V
Substrate	105.324	672.1	-0.914
MAO	432.022	4.740	-0.212
MAO+LSM	962.768	3.465	-0.142

2.4 激光重熔对膜层耐蚀性的影响

铝合金基体、MAO和MAO+LSM膜层的耐蚀实验测试参数见表1。基体的腐蚀电流密度672.1 nA/cm²,腐蚀电位为0.914 V,MAO和MAO+LSM处理后耐蚀性相对基体材料均有大幅提高。MAO膜层的腐蚀电流密度为4.740 nA/cm²,腐蚀电位为0.212 V,激光重熔后腐蚀电流密度和腐蚀电位分别为 3.465×10^{-9} A/cm²和0.142 V,耐蚀性能相对MAO膜层好。膜层的厚度、组织形貌和相组成是影响耐蚀性的重要因素,激光重熔后,膜层的厚度降低了,但致密性好的膜层比例发生显著变化,由疏松层为16~17 μm ,致密层1~2 μm 的MAO膜层变为重熔层7~8 μm ,中间层1~2 μm ,致密层1~2 μm 的LSM+MAO膜层结构,致密膜层比例由10%左右提高至80%左右,有效防腐层显著变厚;重熔对多孔微弧氧化膜层的封孔效果明显,尤其降低了贯穿膜层表面和基体的通孔的几率,另外也增加了耐蚀性能好的 α - Al_2O_3 比例,故激光重熔进一步提高了膜层的耐蚀性能,如图4所示。

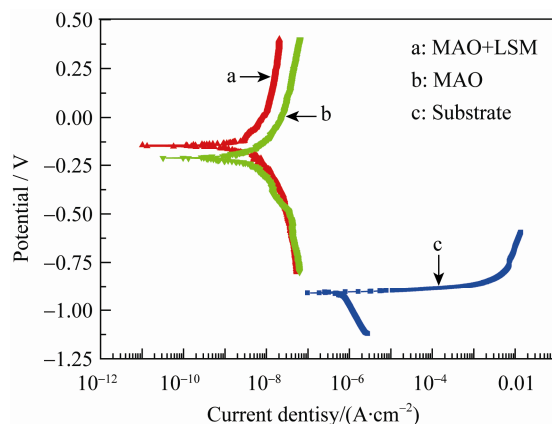


图4 基体、MAO和MAO+LSM膜层的极化曲线图

Fig. 4 Potentiodynamic polarization curves of substrate and MAO, MAO+LSM coatings

3 结论

1) 激光重熔能将MAO膜层表面“火山口”边沿的小突起铺平,微弧放电通道形成的大量微孔被填充,膜层表面变得光滑,微孔稀疏。

2) 激光重熔后,形成了由内往外分别为致密层、中间层和重熔层结构的MAO+LSM膜层。致密层仍为与基体结合力好的MAO膜层,重熔层改变了原MAO外层疏松、多孔的组织,形成了致密、紧凑的膜层,中间层继承了MAO膜层的多孔性,但有所改善,且厚度可控制在整体膜层的20%以下。

3) 激光束辐射的高密度能量促使了膜层中的 $\gamma\text{-Al}_2\text{O}_3$ 向 $\alpha\text{-Al}_2\text{O}_3$ 转变, 提高了膜层的硬度。

4) MAO+LSM 膜层具有致密层和重熔层双层有效防腐膜层, 占到膜层总厚度的 80%以上, 且激光重熔对 MAO 膜层的封孔效果显著, 尤其降低了通孔率, 故 MAO+LSM 膜层较 MAO 表现出更好的耐蚀性能。

参考文献:

- [1] Zuo Y, Zhao P H, Zhao J M. The influences of sealing methods on corrosion behavior of anodized aluminum alloys in NaCl solutions. *Surface and Coatings Technology*, 2003, **166(2/3)**: 237–242.
- [2] Hu J M, Liu L, Zhang J Q, *et al.* Electrodeposition of silane films on aluminum alloys for corrosion protection. *Progress in Organic Coatings*, 2007, **58(4)**: 265–271.
- [3] Ogurtsov N A, Puda A A, Kamarchik P, *et al.* Corrosion inhibition of aluminum alloy in chloride mediums by undoped and doped forms of polyaniline. *Synthetic Metals*, 2004, **143(1)**: 43.
- [4] Nie X, Leyland A, Song H W, *et al.* Thickness effects on the mechanical properties of micro-arc discharge oxide coatings on aluminium alloys. *Surface and Coatings Technology*, 1999, **116**: 1055–1060.
- [5] Wu H H, Wang J B, Long B Y, *et al.* Ultra-hard ceramic coatings fabricated through microarc oxidation on aluminium alloy. *Applied Surface Science*, 2005, **252(5)**: 1545–1552.
- [6] Yerokhin A L, Nie X, Leyland A, *et al.* Plasma electrolysis for surface engineering. *Surface and Coatings Technology*, 1999, **122(2/3)**: 73–93.
- [7] Ko Y G, Lee K M, Shin K R, *et al.* Electrochemical corrosion properties of AZ91 Mg alloy via plasma electrolytic oxidation and subsequent annealing. *Korean Journal of Metals and Materials*, 2010, **48(8)**: 724–729.
- [8] Luo H H, Cai Q Z, Wei B K. Study on the microstructure and corrosion resistance of ZrO_2 -containing ceramic coatings formed on magnesium alloy by plasma electrolytic oxidation. *Journal of Alloys and Compounds*, 2009, **474(1/2)**: 551–556.
- [9] Guan Yong Jun, Xia Yuan, Li Guang. Growth mechanism and corrosion behavior of ceramic coatings on aluminum produced by auto control AC pulse PEO. *Surface and Coatings Technology*, 2008, **202(19)**: 4602–4612.
- [10] Chang S Y, Lee D H, Kim B S, *et al.* Characteristics of plasma electrolytic oxide coatings on Mg-Al-Zn alloy prepared by powder metallurgy. *Metals and Materials International*, 2009, **15(5)**: 759–764.
- [11] Ko Y G, Lee K M, Lee B U, *et al.* An electrochemical analysis of AZ91 Mg alloy processed by plasma electrolytic oxidation followed by static annealing. *Journal of Alloys and Compounds*, 2011, **509(S1)**: S468–S472.
- [12] Sah Santosh Prasad, Tsuji Etsushi, Aoki Yoshitaka, *et al.* Cathodic pulse breakdown of anodic films on aluminium in alkaline silicate electrolyte- Understanding the role of cathodic half-cycle in AC plasma electrolytic oxidation. *Corrosion Science*, 2012, **55**: 90–96.
- [13] Lee Kang Min, Ko Young Gun, Shin Dong Hyuk. Incorporation of carbon nanotubes into micro-coatings film formed on aluminum alloy via plasma electrolytic oxidation. *Materials Letters*, 2011, **65(14)**: 2269–2273.
- [14] Asquith D T, Yerokhin A L, Yates J R, *et al.* Effect of combined shot-peening and PEO treatment on fatigue life of 2024 Al alloy. *Thin Solid Films*, 2006, **515(3)**: 1187–1191.
- [15] Khorasani M, Dehghan A, Shariat M H, *et al.* Microstructure and wear resistance of oxide coatings on Ti-6Al-4V produced by plasma electrolytic oxidation in an inexpensive electrolyte. *Surface and coatings Technology*, 2011, **206(6)**: 1495–1502.
- [16] Dutta-Majumdar J, Manna I. Laser surface alloying of copper with chromium II. Improvement in mechanical properties. *Materials Science and Engineering: A*, 1999, **268(1/2)**: 227–235.
- [17] Amanat N, Chaminade C, Grace J. Transmission laser welding of amorphous and semi-crystalline poly-ether-ether-ketone for applications in the medical device industry. *Material & Design*, 2010, **31(10)**: 4823–4830.
- [18] España Félix A, Ball Vamsi Krishna, Bandyopadhyay Amit. Laser surface modification of AISI 410 stainless steel with brass for enhanced thermal properties. *Surface and Coatings Technology*, 2010, **204(15)**: 2510–2517.
- [19] Wang A H, Wang W Y, Xie C S, *et al.* CO_2 laser-induced structure changes on a zircon refractory. *Applied Surface Science*, 2004, **227(1-4)**: 104–113.
- [20] Harimkar Sandip P, Dahotre Narendra B. Microindentation fracture behavior of laser surface modified alumina ceramic. *Scripta Materialia*, 2008, **58(7)**: 545–548.
- [21] Harimkar S, Dahotre N B. Laser assisted densification of surface porosity in structural alumina ceramic. *Physica Status Solidi (a)*, 2007, **204(4)**: 1105–1113.
- [22] Harimkara Sandip P, Dahotre Narendra B. Characterization of microstructure in laser surface modified alumina ceramic. *Materials Characterization*, 2008, **59(6)**: 700–707.
- [23] Mateos J, Cueto J M, Fernandez E, *et al.* Tribological properties of plasma sprayed and laser remelted 75/25 $\text{Cr}_3\text{C}_2/\text{NiCr}$ coatings. *Tribology International*, 2001, **34(5)**: 345–351.
- [24] Yerokhin A L, Snizhko L O, Gurevina N L, *et al.* Spatial characteristics of discharge phenomena in plasma electrolytic oxidation of aluminium alloy. *Surface and Coatings Technology*, 2004, **177-178**: 779–783.